

# Opto-Mechanics of deformable Fabry-Pérot Cavities

Constanze Metzger,<sup>\*</sup> Ivan Favero,<sup>†</sup> Alexander Ortlieb, and Khaled Karrai<sup>‡</sup>  
*Center for NanoScience and Fakultät für Physik, Ludwig-Maximilians-Universität,  
Geschwister-Scholl-Platz 1, 80539 München, Germany*

(Dated: June 11, 2021)

## Abstract

We investigated the opto-mechanical properties of a Fabry-Pérot cavity with a mirror mounted on a spring. Such a structure allows the cavity length to change elastically under the effect of light induced forces. This opto-mechanical coupling is exploited to control the amplitude of mechanical fluctuation of the mirror. We present a model developed in the classical limit and discuss data obtained in the particular case for which photo-thermal forces are dominant.

## I. INTRODUCTION

Photo-induced forces acting on a spring-mounted mirror are known to affect its dynamics<sup>1,2,3,4,5,6,7,8,9,10,11,12,13,14,15,16,17,18</sup>. We built a miniature Fabry-Pérot (FP) cavity with a moveable mirror held on a spring while the other mirror was massive enough to be static. The flexible mirror is compliant so that it moves under the influence of light-induced forces originating from radiation pressure or photothermal forces that build up in the cavity. Such forces depend on the light intensity stored in the cavity, and their exact magnitude is determined by the cavity's mirror separation in proportion to the optical FP resonances. Consequently, any displacement of the mirror, resulting for example from thermal fluctuations, leads to a change in the light-induced force, inducing in return a change in the mirror position. This opto-mechanical coupling is referred to as intrinsic light-induced back-action<sup>1</sup>.

An optical back-action mechanism shifting the resonance frequency and adding damping on a mechanical resonator was first reported by V.B. Braginsky<sup>1</sup> three decades ago. Optical back-action remained a field of interest, especially in the research area of gravitational wave detection<sup>2,3</sup>. Gravitational wave detectors, mostly Michelson interferometers (for example LIGO, a Michelson interferometer with arm lengths of 4 km that is illuminated with a 6 W Nd:YAG laser beam<sup>19</sup>), are prone to get unstable because of optical back-action. Instabilities were reported as well in smaller scale systems. A centimeter sized mirror hung on strings and serving as one mirror of a FP cavity showed mechanical instability under few Watts of illumination<sup>5</sup>. More recently, back-action was reported in microscale systems<sup>9,18</sup>. When the photon back-action force is delayed in time with respect to changes in mirror position, additional dissipation in the mirror's motion occurs without adding any additional mechanical fluctuations. The enhanced dissipation leads to reduced vibrational fluctuation and temperature of the mirror<sup>4,7,8,9,10</sup>, a situation referred to as passive optical cooling<sup>4</sup>. Quantum mechanical behavior of a miniature mirror is expected<sup>6</sup> when the optical cooling becomes efficient enough to cool the mirror near its vibrational ground state. Experiments using a combination of photo-thermal forces and radiation pressure to cool a micromirror passively reach a temperature range of about 10 K in references<sup>4,7,8</sup>. Optical cooling dominated by radiation pressure has been demonstrated not only in FP cavities<sup>7,8</sup> but in silica microtoroids<sup>9</sup> with a diameter in the range of 100  $\mu\text{m}$  as well. Unfortunately, optical cooling mechanisms start to become inefficient as soon as the mirror reaches size smaller than the diffraction limit of light in the cavity. Nevertheless, cooling of a micromirror with a diameter in the range of the laser wavelength was recently successfully demonstrated<sup>10</sup>. In analogy to optical cooling, capacitive cooling of a nano-mechanical resonator through charge coupling with a superconducting single-electron-transistor was shown<sup>20</sup>. For a reviewpaper see ref<sup>21</sup>.

In a pioneering work and in contrast to passive cooling mechanisms, Cohadon, Heidmann and Pinard demonstrated the possibility of optical active cooling using an external electronic feedback loop in their system<sup>11</sup>. In an earlier set of data by Mertz and coworkers<sup>12</sup>, optical induced damping by active feedback was observed. In cold damping schemes, a laser beam

is directed towards the flexible mirror and can displace it exerting radiation pressure<sup>11</sup> or a photo thermal force<sup>12</sup>. The velocity of the mirror is detected and the laser intensity is adjusted by an electronic feedback loop in an appropriate way<sup>13,14</sup>. In principle, because this technique modulates the light intensity in proportion to a signal derived from the mirror amplitude noise, it adds technical fluctuations in the system. Using active optical cooling, up to now effective temperatures as low as 135 mK could be reached<sup>15</sup> with a cantilever starting from room temperature. Recently, active cooling of a cantilever from 2.2 K down to about 3 mK was observed<sup>17</sup> using not optical but electrostatic feedback forces. In this paper, we present a model describing passive optical cavity cooling in a classical approximation and report on the passive cavity cooling of a micromirror by photo-thermal back-action forces under various experimental conditions.

In chapter II, we present solutions to the equation of motion of a mirror with a delayed light-induced force acting on it. A derivation of the vibrational temperature of a mirror cooled by photo-induced forces is given in chapter III. Chapter IV describes the mirror's equation of motion under a weakly modulated light-induced force. Different micro FP experiments giving rise to optical cooling are presented in chapter V and VI. Finally, in chapter VII we compare the cooling power for different light induced forces. We discuss the possibility that cooling by photo-thermal effects allows reaching lower temperatures compared to cooling by radiation pressure.

## II. EQUATION OF MOTION UNDER CONSTANT ILLUMINATION

In this chapter, we solve the equation of motion of a vibrating harmonic oscillator forming a mirror of a FP cavity in the limit of small vibrational amplitudes. In our setup, a laser beam is coupled into the cavity through a fixed semi-transparent input mirror. Depending on the mirror distance, a resonance builds up in the cavity. The photons stored in the deformable FP cavity exert a force  $F_{ph}$  on the compliant mirror originating on the light-field present in the cavity. The force can be any photon-induced force such as radiation pressure, photo-thermal deformation of the mirror, radiometric pressure or else. For sake of generality  $F_{ph}$  in our analysis is assumed to be any possible photon induced force that is proportional to the local light intensity at the location of the mirror. Generally such forces do not respond instantaneously at a change in mirror position, but only delayed after a characteristic time constant  $\tau$ . For example, the finite photon storage time of a cavity accounts for the delay of radiation pressure forces with respect to a change in cavity length, while photo-thermal action on the mirror is retarded by the time it takes to conduct heat conduction along the cantilever. A model system with a mirror that is able to move under the influence of a delayed photon force is shown in FIG.1 (a).

We consider the equation of motion for the center of mass position  $z$  of a oscillator with an effective mass  $m$ , mechanical damping  $\Gamma$  and spring constant  $K$ . The mirror thermal

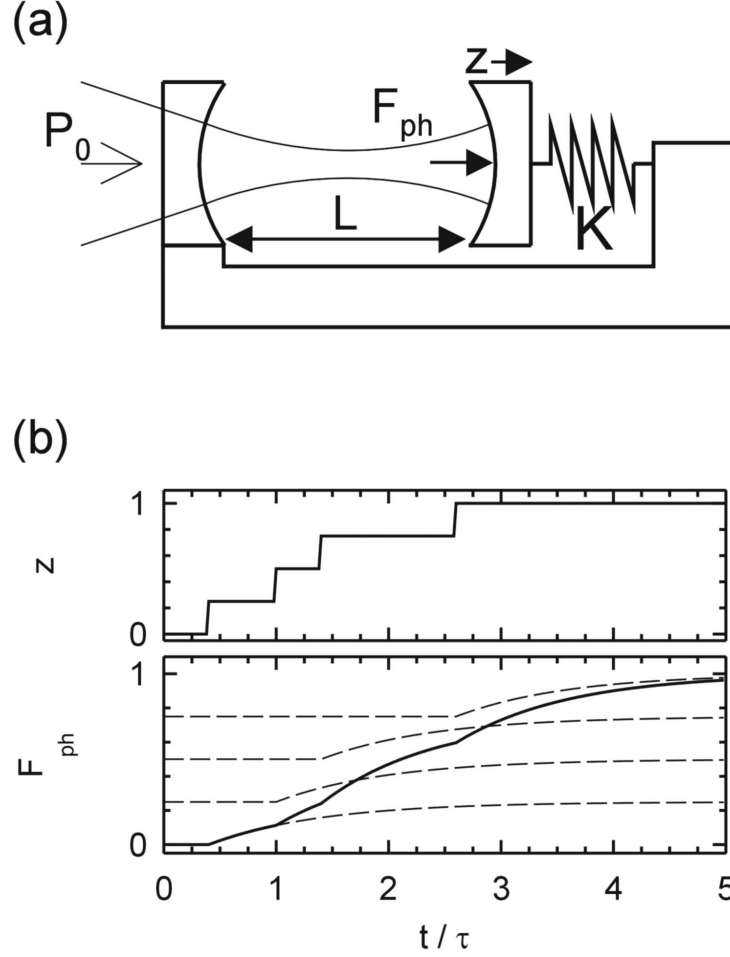


FIG. 1: (a) schematic model of a deformable Fabry-Pérot cavity. (b) After discrete step-shaped changes in mirror distance  $z$ , the light-induced force  $F$  grows after a characteristic delay time  $\tau$ .

fluctuations are assumed to be driven by an thermal Langevin Force  $F_{th}$ .

$$m\ddot{z}(t) + m\Gamma\dot{z}(t) + Kz(t) = F_{th}(t) + F_{ph}(z(t)) . \quad (1)$$

In the following, we model the total light induced force on the cantilever. To illustrate, we consider that the cantilever position fluctuates in random increments under the effect of thermal excitations. The photon force responds retarded in time. After a step of  $z_n - z_{n-1}$  at time  $t_n$ , the light-induced force  $F_{ph}$  follows with the delay time  $\tau$  as depicted in FIG. 1 (b). If we were to stop the random motion of the mirror at step  $n$ , the light-induced force would reach asymptotically the static value  $F(z_n)$ . To model the behavior of  $F_{ph}(z(t))$  after  $N$  steps in mirror position we sum up all force increments such

$$F_{ph}(z_N(t)) = F(z_0) + \sum_{n=1}^N h(t - t_n)[F(z_n) - F(z_{n-1})] \quad (2)$$

where the function  $h(t)$  describes the time delay. This discrete sum can be reformulated as a continuous integral in time

$$F_{ph}(z(t)) = F(z_0) + \int_0^t dt' \frac{dF(z(t'))}{dt'} h(t - t'). \quad (3)$$

The equation of motion we need to solve then reads as

$$m\ddot{z}(t) + m\Gamma\dot{z}(t) + Kz(t) = F_{th}(t) + F(z_0) + \int_0^t dt' \frac{dF(z(t'))}{dt'} h(t - t'). \quad (4)$$

This equation<sup>4</sup> leads to complex dynamics with multi-stability points treated in a recent work by F. Marquardt and coworkers<sup>16</sup>. Here we focus on optical cooling, so for all practical purpose we assume the mirror amplitudes to be small compared to the change in cavity length needed for the optical resonance condition to change substantially. In terms of the FP cavity finesse  $F = (\pi/2)g$  with  $g = 2\sqrt{R}/(1 - R)$  this constraint translates into  $z \ll \lambda/(2\pi g)$  where  $R$  is the reflectivity of the cavity mirrors.

Equation (4) is solved by Laplace transform, which is defined for a function  $f(t)$  as

$$f_\omega = \int_0^\infty dt f(t) e^{-i\omega t}. \quad (5)$$

The constant force term  $F(z_0)$  in eq. (4) has no time dependence and simply leads to a static shift of the oscillator's average position. By selecting the new average position for  $z$  it can be dropped from eq. (4). The Laplace transform of eq. (4) yields

$$-m\omega^2 z_\omega + i\omega m\Gamma z_\omega + Kz_\omega = \int_0^\infty dt e^{-i\omega t} \left[ F_{th}(t) + \int_0^t dt' \frac{dF(z(t'))}{dt'} h(t - t') \right] \quad (6)$$

As  $F(z(t'))$  depends on time indirectly through  $z(t')$ , its derivative in eq.(6) is rewritten as

$$dF(z(t'))/dt' = \frac{\partial F(z(t'))}{\partial z} \frac{\partial z(t')}{\partial t'}. \quad (7)$$

In accordance with the small amplitude approximation,  $F(z(t'))$  is developed in a Taylor expansion around  $z(t_0)$ :  $F(z(t')) \approx F(z(t_0)) + [z(t') - z(t_0)]\nabla F$  where we used the abbreviation  $\partial F(z(t'))/\partial z|_{z=z(t_0)} = \nabla F$ . In the small amplitude fluctuation approximation, the partial derivative  $\partial F(z(t'))/\partial z$  is now approximated with  $\nabla F$ . We can reformulate eq. (6) as follows

$$-m\omega^2 z_\omega + i\omega m\Gamma z_\omega + Kz_\omega = F_{th,\omega} + \int_0^\infty dt e^{-i\omega t} \left[ \int_0^t dt' \nabla F \frac{\partial z(t')}{\partial t'} h(t - t') \right]. \quad (8)$$

With the property of Laplace transform for convolutions

$$\int_0^\infty dt e^{-i\omega t} \left[ \int_0^t dt' f_1(t') f_2(t - t') \right] = f_{1,\omega} f_{2,\omega} \quad (9)$$

eq. (8) is reformulated as

$$-m\omega^2 z_\omega + i\omega m\Gamma z_\omega + Kz_\omega = F_{th,\omega} + \nabla F i\omega z_\omega h_\omega. \quad (10)$$

We assume that the shape of the delay function is of exponential type

$$h(t) = 1 - e^{-t/\tau}. \quad (11)$$

This is reasonable, because  $h(t)$  describes the timescale the cavity system needs to approach a new equilibrium state after a disturbance. For instance radiation pressure reacts with an exponential behavior. The other process considered in this work, the heat flow in an absorbing mirror after a change of cavity length, has an exponential response as well. The Laplace transform of the response function  $h(t)$  is given by

$$h_\omega = \frac{1}{i\omega(1 + i\omega\tau)}. \quad (12)$$

The terms on the right hand side of eq. (10) can be regrouped in powers of  $\omega$  and eq. (10) is rewritten as

$$-m\omega^2 z_\omega + i\omega m \Gamma_{\text{eff}} z_\omega + K_{\text{eff}} z_\omega = F_{th,\omega} \quad (13)$$

with an effective damping

$$\Gamma_{\text{eff}} = \Gamma \left( 1 + Q_M \frac{\omega_0 \tau}{1 + \omega^2 \tau^2} \frac{\nabla F}{K} \right) \quad (14)$$

and an effective spring constant

$$K_{\text{eff}} = K \left( 1 - \frac{1}{1 + \omega^2 \tau^2} \frac{\nabla F}{K} \right). \quad (15)$$

In eq. (14), we used the vibrational harmonic resonance frequency of the center of mass of the mirror  $\omega_0^2 = K/m$  and we defined the mechanical quality factor such that

$$Q_M = \frac{\omega_0}{\Gamma}. \quad (16)$$

Both the effective damping and rigidity are unusual in that they now include a frequency dependent term. The frequency dependency is that of a low-pass filter that ensures that at very high frequencies the retarded back-action has no effect on the properties of the harmonic oscillator. Above cut-off the oscillating mirror behaves as if it was placed in the dark. In the limit of low frequencies (static limit) the effective damping and spring rigidities are constant and as a result the solution of the equation of motion is that of an harmonic oscillator with optically modified frequencies and quality factor. For applications involving laser cooling of the lowest mechanical vibrational mode, the frequency range of interest is  $\omega \approx \omega_0$ , the cantilever's resonance frequency. We define the effective resonance frequency

$$\omega_{\text{eff}}^2 = \omega_0^2 \left( 1 - \frac{1}{1 + \omega^2 \tau^2} \frac{\nabla F}{K} \right). \quad (17)$$

where  $\omega_{\text{eff}}^2 = K_{\text{eff}}/m$ . The solution for the amplitude in the frequency domain of the harmonic oscillator is

$$z_\omega = \frac{F_{th,\omega}}{m} \frac{1}{\omega_{\text{eff}}^2 - \omega^2 + i\omega\Gamma_{\text{eff}}}. \quad (18)$$

It is important to note that we did not take into account that  $h(t)$  is a function of the cavity detuning in contrast to the model in ref<sup>8</sup>. In our simplified approach with low finesse cavities the effect of detuning on  $h(t)$  is not measurable but becomes significant at high finesse<sup>8,9</sup>. The delay time of photo-thermal forces is entirely determined by heat conduction in the mirror and is not dependent on cavity detuning at all.

### III. EFFECTIVE TEMPERATURE

In thermodynamical equilibrium without illumination and any light-induced effects, the average power in the mechanical ground mode of the mirror center of mass motion is described by the equipartition theorem:

$$\frac{1}{2}K \int_0^\infty dt |z_{\text{dark}}(t)|^2 = \frac{1}{2}k_B T. \quad (19)$$

Here  $k_B$  is Boltzmann's constant and  $T$  the bath temperature. An important property of Laplace transforms is that the integrated Laplace coefficients  $\int d\omega |z_\omega|^2$  equals the time average

$$\int_0^\infty d\omega |z_{\text{dark},\omega}|^2 = \int_0^\infty dt |z_{\text{dark}}|^2. \quad (20)$$

This expression provides the prescription for performing vibrational thermometry, namely a method to extract a temperature from the measurement of the spectral distribution of the Brownian motion of the mirror. First the rigidity  $K$  must be determined independently, for instance by measuring the resonance frequency knowing the oscillator effective mass, then the spectrum of the fluctuation amplitude  $z_\omega$  is measured on a sufficiently extended frequency range around the vibrational resonance frequency and averaged over a large enough number of measurements. Finally the integration of  $|z_\omega|$  multiplied by the rigidity gives the thermal energy experienced by the harmonic oscillator and hence the temperature. We will use this prescription later on to determine the temperature of the mirror coupled to the optical cavity. The expression for the frequency averaged square modulus of the amplitude can be now computed using the solution  $z_\omega$  of eq. (18) but still as a function of the still non-explicitly expressed thermal fluctuation force component  $F_{th,\omega}$ . In absence of light in the cavity the equipartition theorem gives us already the opportunity to derive the expression of  $F_{th,\omega}$  that we can then finally use to obtain the dynamics of the mirror with light in the cavity. As we will see shortly, the result will be that the mirror fluctuates in a way nearly identical to the Brownian motion of the original harmonic oscillator in dark but with a modified temperature induced by the presence of light in the cavity. In dark, setting all light induced effects to zero in eq. (1) for  $z_\omega$ , we have

$$z_{\text{dark},\omega} = \frac{F_{th,\omega}}{m} \frac{1}{\omega_0^2 - \omega^2 + i\omega\Gamma}. \quad (21)$$

With the reasonable assumption that the spectral force density of thermal vibrations given by  $F_{th,\omega}$  are equally distributed over all frequencies, one can calculate the strength of the

thermal force. We assume that

$$|F_{th,\omega}|^2 = Sdf \quad (22)$$

in every frequency interval  $df$  with a constant spectral density  $S$  which can be calculated in the next step by integrating eq. (21) over all frequencies  $\omega$

$$\int_0^\infty d\omega |z_{\text{dark},\omega}|^2 = \int_0^\infty d\omega \frac{S}{2\pi m^2} \frac{1}{(\omega_0^2 - \omega^2)^2 + \omega^2 \Gamma^2}. \quad (23)$$

The experimentally relevant assumption  $\Gamma \ll \omega_0$  is made, so the integral simplifies to

$$\int_0^\infty d\omega |z_{\text{dark},\omega}|^2 = \frac{S}{2\pi m^2 \Gamma^2 \omega_0^2} \int_0^\infty d\omega \frac{1}{4\left(\frac{\omega_0 - \omega}{\Gamma}\right)^2 + 1}. \quad (24)$$

leading to the solution

$$\int_0^\infty d\omega |z_{\text{dark},\omega}|^2 = \frac{S}{4K\Gamma m}. \quad (25)$$

With that result, the solution of the oscillator's spectrum eq. (25) can be inserted in the equipartition theorem eq. (19). The driving fluctuation eq. (22) is determined:

$$|F_{th,\omega}|^2 = 4k_B T m \Gamma \frac{d\omega}{2\pi}. \quad (26)$$

Finally the thermal noise spectrum of a harmonic oscillator in the dark is

$$|z_{\text{dark},\omega}|^2 = \frac{4k_B T \Gamma}{m} \frac{1}{(\omega_0^2 - \omega^2)^2 + (\omega \Gamma)^2} \frac{d\omega}{2\pi}. \quad (27)$$

Now, we still need to find an expression for the thermal driving force  $F_{th,\omega}$  in the solution of the equation of motion with light eq. (18). When the light is turned on, the spectral force density  $F_{th,\omega} = Sdf$  is not influenced by the photon induced force and eq. (26) still holds, because it is only dependent on the natural mechanical damping  $\Gamma$  and the undisturbed spring constant  $K$ . The spectral amplitude of a mirror under illumination is

$$|z_\omega|^2 = \frac{4k_B T \Gamma}{m} \frac{1}{(\omega_{\text{eff}}^2 - \omega^2)^2 + (\omega \Gamma_{\text{eff}})^2} \frac{d\omega}{2\pi}. \quad (28)$$

Integrating this over all frequencies and using the property of Laplace transforms eq. (20) gives

$$\int_0^\infty dt |z|^2 = \frac{\Gamma}{\Gamma_{\text{eff}}} \frac{k_B T}{K_{\text{eff}}}. \quad (29)$$

This averaged squared amplitude is related to a temperature  $T_{\text{eff}}$  via the equipartition theorem:

$$\frac{1}{2} K_{\text{eff}} \int_0^\infty dt |z|^2 = \frac{1}{2} k_B T_{\text{eff}}. \quad (30)$$

Solving this for the effective temperature and using eq. (29) yields

$$\frac{T_{\text{eff}}}{T} = \frac{\Gamma}{\Gamma_{\text{eff}}}. \quad (31)$$



No absorption of light in the mirror was taken into account up to now. Still even dielectric mirrors possess a residual absorption leading to heating. If the temperature is increased considerably above the bath temperature, eq. (31) needs to be corrected. The bath temperature  $T$  has to be substituted then with the temperature the mirror would reach in absence of optical cooling  $T + \Delta T$ .

In a previous work<sup>4</sup>, we established that  $T_{\text{eff}}/T = (\Gamma/\Gamma_{\text{eff}})(K/K_{\text{eff}})$  which does not take into account that the effective temperature is determined by the squared noise amplitude  $\int_0^\infty dt |z|^2$  multiplied with the independently measured effective spring constant  $K_{\text{eff}}$  instead of the unperturbed spring constant  $K$ . This correction creates a factor  $K_{\text{eff}}/K$  yielding the effective temperature eq. (31).

With the help of eq. (14), the result of eq. (31) is reformulated as

$$\frac{T_{\text{eff}}}{T} = \frac{1}{1 + Q_M \frac{\omega_0 \tau}{1 + \omega^2 \tau^2} \frac{\nabla F}{K}} \quad (32)$$

revealing the physical parameters playing a role in cavity cooling.

The cooling stops when the static spring constant  $K_{\text{eff}}(\omega = 0)$  reaches zero and becomes negative. At this point, mirror bistability sets in<sup>18</sup> and no stable measurement is possible any more. Consequently, a theoretical limit of cooling is obtained for  $K_{\text{eff}} = K(1 - \nabla F/K) = 0$  in eq. (32) and considering the optimal case of  $\omega_0 \tau = 1$

$$\frac{T_{\text{eff,Limit}}}{T} = \frac{1}{1 + Q_M/2}. \quad (33)$$

This expression shows that the mechanical quality factor  $Q_M$ , which relates to the ability of the mechanical mode to dissipate its energy, plays a central role for the optical cooling mechanism.

According to eq. (31) the lowest effective temperature is entirely driven by the damping modified through the cavity effect. In turn this modification in damping exists only if a time delay exists between the motion of the mirror and the resulting change in the light induced force it experiences, see eq. (14). So the essence of optical cooling finds its root on the retarded back-action on the mirror displacement.

Up to now, we did not offer an explanation as to where the thermal energy extracted from the vibrating cantilever goes. It turns into fluctuation of the electromagnetic field escaping the cavity as shown in FIG. 2. The system formed by the mechanical oscillator and the electromagnetic field remains at constant temperature. We offer a possible picture on how this happens. The fluctuating cavity length modulates the photon frequency at all frequencies but with amplitude maxima at the vibrational resonance frequency. Such amplitude modulation of the light-field produces side bands above and below the photon frequency with peaks shifted on both sides by the vibrational resonance of the mirror (in Raman spectroscopy they would be Stokes and anti-Stokes resonances). When the laser is red detuned from the cavity transmission maximum, the band with shorter wavelength is closer to the transmission peak. Seen from the outside world a detector would measure a fluctuating irradiance imbalance between the side bands as more blue shifted light is

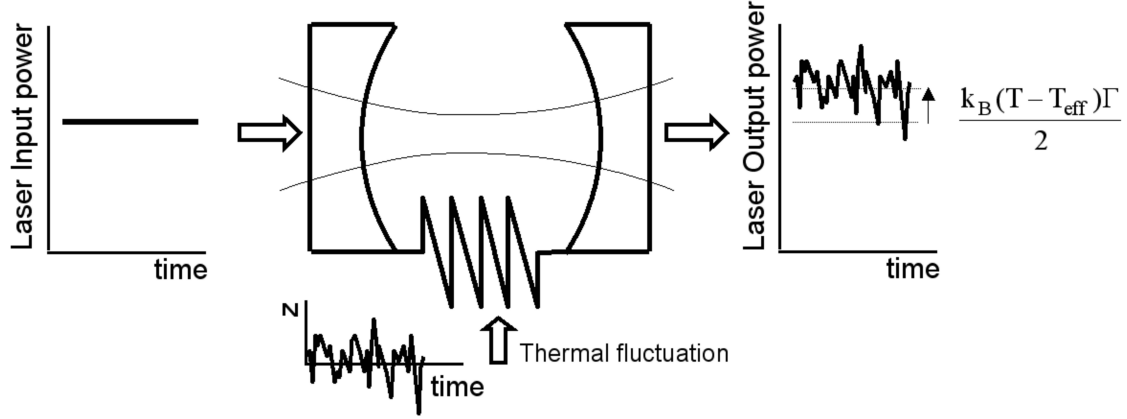


FIG. 2: A FP cavity with a mirror attached on a spring is illuminated with a laser beam. The input laser intensity is assumed to be noiseless. The transmitted light shows amplitude fluctuations, that are impressed on the original amplitude by the thermal fluctuation of the mirror. More importantly, the transmitted laser light has an averaged intensity enhanced by the fluctuations added by the mechanical resonator. The mirror vibrational motion has been cooled and the excess energy turns into photons.

reaching the detector than red shifted. This excess of energy is given by the difference in transmitted light power between the blue and red side of the band and this over the typical delay time constant for the light induced force to correct against the mirror fluctuation. The excess energy has been taken away from the very source that produced the side bands to begin with, namely from the Brownian fluctuation of the mirror. In this picture, the cooling is optimal when the frequency width of the cavity, that is the inverse storage time  $1/\tau$ , is comparable to the side-band frequency separation from the laser light frequency, in other words when  $\omega_0\tau \approx 1$ . This picture seems to be consistent with the model and in particular it is easy to see that with a zero time delay the net excess energy is also zero and no cooling is possible. An alternative picture possibly more appropriate to photo-thermal cooling is the following. The laser light is tuned to be red-shifted from a transmission peak of the cavity. When the cavity length fluctuates and say becomes shorter over a certain time period, the transmission peak gets closer to the laser line and more light can be stored in the cavity during that time. The result of the excess light is to exert more pressure on the mirror as to oppose the cavity from becoming even shorter. In the opposite case, when the cavity gets longer upon a thermal fluctuation, the averaged steady state light pressure that displaced the mirror from its position in dark reduces and the mirror tends to move back under its own restoring elastic force as to oppose this very fluctuation. The retarded back-action makes this force oppose the mirror velocity  $dz/dt$  and not only its instantaneous position  $z$ . It is therefore a dissipative force and during the typical response time, energy is irreversibly lost to the light field outside the cavity. In this picture the cavity

serves as a reservoir of energy stored in form of light, and the rate of energy leakage from this reservoir is fully controlled by the mirror kinetics. Energy conservation dictates that mechanical energy can be transformed into energy that escapes the reservoir in form of light.

#### IV. EQUATION OF MOTION UNDER MODULATED ILLUMINATION

The solution of the equation of motion of a mirror under the influence of light-induced forces of chapter II is generalized for a weakly modulated light-induced force. This modification proves to be useful, because a measurement with modulated laser light opens up the possibility to measure the magnitude of the light-induced force as well as its delay time. The technique makes it possible to determine if either radiation pressure, photo-thermal pressure or even a summation of both effects are responsible for the observed cooling effects. We took advantage of this method in a modulated laser measurement that is discussed in chapter V.

If the laser intensity is weakly modulated, the light-induced force is described by

$$F(z(t), t) = (1 + \varepsilon(t))F_{ph}(z(t)) \quad (34)$$

with a small modulation strength  $\varepsilon(t) \ll 1$ . The light-induced force has now an explicit dependence on  $t$  and differs from eq. (3) as follows

$$F(z(t), t) = F_{ph}(z_0) + \int_0^t \left( \frac{\partial F_{ph}}{\partial t'} + \frac{\partial F_{ph}}{\partial z} \frac{\partial z}{\partial t'} \right) h(t - t') dt'. \quad (35)$$

The solution for the amplitude is:

$$z_\omega = \left( \frac{F_{th,\omega}}{m} + \frac{F_{ph}}{m} \frac{\varepsilon_\omega}{1 + i\omega\tau} \right) \frac{1}{\omega_{\text{eff}}^2 - \omega^2 + i\omega\Gamma_{\text{eff}}}. \quad (36)$$

Compared to the solution without external excitation of the mirror eq. (18), the amplitude has an additional term  $(F_{ph}/m) \varepsilon_\omega / (1 + i\omega\tau)$ . This term offers a way to extract both the delay time  $\tau$  and the magnitude of the light-induced force  $F_{ph}$  from a measurement of the real part as well as the imaginary component of the response  $z_\omega$  so the measurement can be done with the aid of lock-in detection (see chapter V) by measuring the in and out of phase component of the reflected light. Using eq. (36) to model the data, the delay time of the force is extracted. Besides, if different light-induced forces like radiation pressure and photo-thermal pressure are present in the setup, the ratio of different forces can be determined when their response times differ significantly.

In the next two chapters, we are investigating in two different setups for the optical cooling of the vibration modes of a gold coated AFM silicon cantilever. In this system, the presence of the bilayer gives rise to a photo-thermal bending of the lever under illumination. The delay time of the light-induced force is the time of thermal response of the lever.

## V. COOLING OF THE GROUND MODE

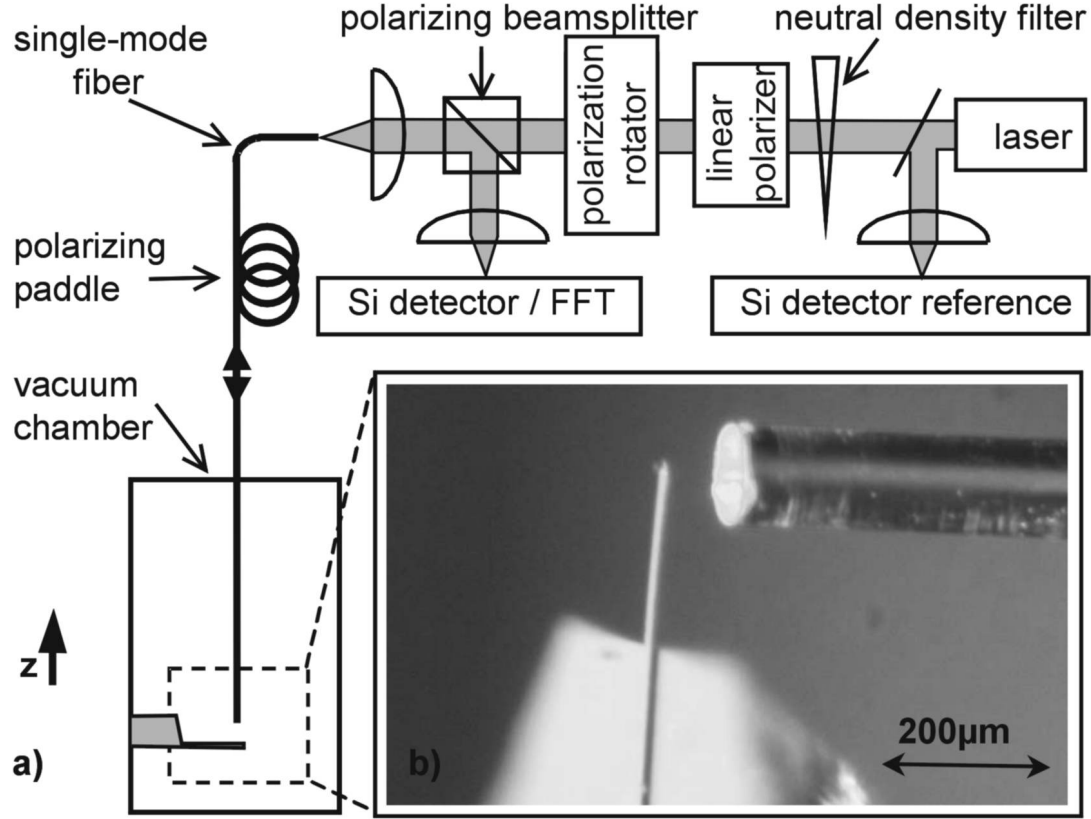


FIG. 3: (a) Schematic of the experimental setup. Inset (b) shows a photograph of a similar cavity as used in the experiment but with a lever to mirror separation greatly increased for the picture. During measurements, the cavity length was  $34 \mu\text{m}$ .

In this chapter, a setup displaying passive back-action cooling is shown (see FIG. (3)). We used alternatively a red HeNe-laser (Research electro optics LHRP 1701,  $\lambda = 632.8 \text{ nm}$ , 17 mW) or a diode laser ( $\lambda = 670 \text{ nm}$ , 5 mW) beam coupled into a single mode optical fiber (numerical aperture 0.13). The highly coherent HeNe laser was used for the vibrational resonance linewidth measurements shown in FIG. 5. For measurements involving laser amplitude modulation, we preferred using the diode laser because it could be easily modulated. A neutral density filter wheel allowed tuning the laser power continuously over almost four orders of magnitude. The reflected laser power was measured at the level of the Si detector was varied from 35 nW to up to  $150 \mu\text{W}$ . The fiber was introduced into a vacuum chamber operating down to a pressure in the  $10^{-6}$  mbar range. Reaching this low enough pressure was important in order to reduce the damping of the cantilever as shown later in FIG. 5 (a). The fiber end forming a cavity mirror in the vacuum chamber was thoroughly polished and coated with a gold film of 19 nm by thermal evaporation under high vacuum. A silicon

cantilever (Nanosensors) with a width of  $22\text{ }\mu\text{m}$ , a thickness of  $0.47\text{ }\mu\text{m}$ , a length of  $220\text{ }\mu\text{m}$  and a spring constant of  $0.008\text{ N/m}$  was mounted at a distance of  $34\text{ }\mu\text{m}$  of the polished fiber end. Gold layers of  $36\text{ nm}$  were deposited on each side of the lever. A simulation of the coated cantilever optical properties gave a reflectivity of 82% for a laser wavelength of  $633\text{ nm}$ . The distance between fiber and cantilever was tuned by applying a DC-voltage between them to create a capacitive force. About  $15\text{ V}$  were required in order to detune the cavity through three resonances. The light reflected from the cavity was coupled back into the fiber. A fiber paddle polarizator was used to rotate the linear polarization of the reflected light in order to be directed by a polarizing beamsplitter onto a Si-photodetector and minimize back reflected light on the laser. We increased this way the collected efficiency by a factor four. For additional isolation we used a polarization rotator ( $\lambda/2 \pm 1\%$  Fresnel rhombus, B. Halle Nachf., 400-700 nm) rotating the linear laser polarization by  $45^\circ$  per pass and a linear polarizer (Glan-Thompson, isolation 50 dB) before fiber coupling.

In FIG. 4 (a), the normalized reflectivity of the FP cavity is shown. The cavity finesse is about four, which corresponds to  $g = 2.5$ . FIG. 4 (b) shows spectra of the cantilever fundamental harmonic at  $7.3\text{ kHz}$  with effective temperatures of  $300\text{ K}$ ,  $86\text{ K}$ ,  $64\text{ K}$ ,  $32\text{ K}$  respectively. All curves are taken at the same cavity detuning of  $\Delta z = +\lambda/(2\pi g\sqrt{3}) \approx \lambda/25$  for which one expects maximum gradient of the light-induced force, and therefore maximum cavity cooling<sup>18</sup>. At very low reflected laser power of  $3.1\text{ }\mu\text{W}$  one measures the amplitude fluctuation spectral density near vibrational resonance of the cantilever corresponding to a temperature of  $300\text{ K}$ . A fit with eq. (27) is obtained with the parameters  $f = 7265\text{ Hz}$ ,  $K = 2.5 \times 10^{-2}\text{ N/m}$ ,  $\Gamma = 28\text{ Hz}$ . At increased laser power of  $3.6\text{ mW}$  the effective damping is found to be  $\Gamma_{\text{eff}} = 263$  which relates using eq. (31) to an effective temperature of  $32\text{ K}$  for this set of data. So far the lowest temperature obtained with this setup<sup>4</sup> was  $18\text{ K}$ . In order to achieve highest possible cooling effect, different parameters have to be optimized as stated in eq. (32).

First, the mechanical damping  $\Gamma$  of the cantilever needs to be minimized. The damping of a resonator includes several contributions such as clamping losses, defects in crystal structure, surface losses<sup>22</sup> and damping due to scattering of air molecules to name a few. The latter can be reduced by running the system in vacuum. A simple model of the gas damping can be found by assuming that the viscous damping by molecular scattering is  $F_{\text{visc}} = (Nm_N v)/t_{\text{scat}}$  with  $N$  the number of atoms scattering off the cantilever,  $m_N = 4.6 \times 10^{-26}\text{ kg}$  the mass of nitrogen atoms,  $v = 510\text{ m/s}$  the mean atomic velocity at  $300\text{ K}$  and  $t_{\text{scat}}$  the mean scattering time. This approximation predicts that at a pressure of  $10^{-3}\text{ mbar}$  already molecular scattering should account for 1% of the damping. In reality, we still see a sizeable change in quality factor going from  $10^{-3}\text{ mbar}$  ( $\Gamma = 61.7\text{ Hz}$ ) to  $5 \times 10^{-6}\text{ mbar}$  ( $\Gamma = 14.5\text{ Hz}$ ). The linewidth at full width half maximum FWHM relates to the mechanical damping such as  $\text{FWHM} = \sqrt{3}\Gamma/(2\pi)$ . We find a linewidth of  $17\text{ Hz}$  corresponding to a quality factor of  $Q_M = 744$  for  $10^{-3}\text{ mbar}$  and a linewidth of  $4\text{ Hz}$  ( $Q_M = 3161$ ) for  $5 \times 10^{-6}\text{ mbar}$  as shown in FIG. 5 (a) at low reflected power. Evidently, the observed damping cannot be explained by molecular viscous damping alone. Molecular adsorption on the cantilever surface may

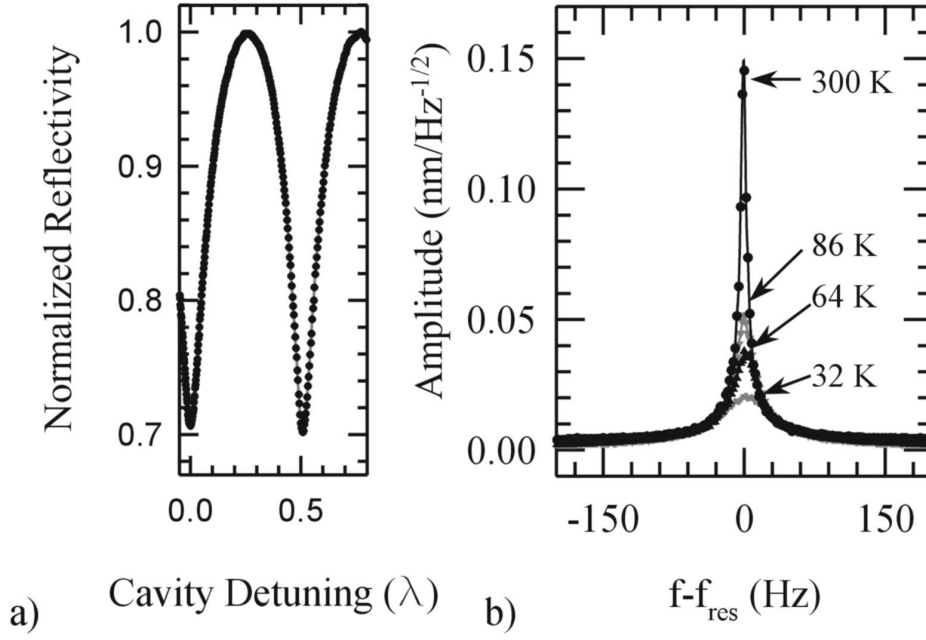


FIG. 4: (a) Normalized reflectivity of plan-plan cavity setup shown in FIG. 3. The cavity detuning is calibrated in units of the wavelength  $\lambda$ . The Finesse is 4, with the parameter  $g=2.5$ . (b) Amplitude fluctuation spectral density near vibrational resonance of the cantilever with  $f_0 = 7.3$  kHz with different laser powers taken at cavity detuning of  $+\lambda/25$  from a cavity resonance. The largest amplitude corresponds to thermal fluctuation at 300 K with mechanical damping  $\Gamma = 28$  Hz, measured with reflected laser power of  $3.1\mu\text{W}$ . The other measurements correspond to reflected laser powers of 0.87 mW, 1.3 mW, and 3.6 mW with damping of  $\Gamma = 98$  Hz, 131 Hz, and 263 Hz. The effective temperatures of the spectra are from top to bottom 300 K, 86 K, 64 K, and finally 32 K.

be responsible for the additional damping so at lower pressure desorption could explain the improved quality factor. As seen in eq. (14), the linewidth of the mechanical resonance is modified linearly with laser power as long as the photon-induced force is linear with intensity. In the cooling regime, it is broadened with increasing laser power starting from the natural linewidth at dark. In FIG. 5 (a) the linear dependency of the linewidth with the reflected laser power is plotted in logarithmic scale for different chamber pressures, showing smallest possible linewidth at low pressure and low laser power.

In order to maximize the cooling efficiency, a tradeoff between the reflectivity of the cantilever and its mechanical damping had to be made. Higher reflectivity should increase the

cavity finesse and therefore lead to stronger cooling effect, through both an increase of the light power circulating in the cavity close to resonance and an increase of its gradient upon position. Unfortunately, increasing the reflectivity by evaporating a thicker gold layer on the cantilever adds additional mechanical damping as well<sup>23</sup>. In our experiment we used different thicknesses of evaporated gold on many cantilevers of the same kind, the quality factor decreased by an order of magnitude as shown in FIG. 5 (b).

Second, to enhance the cooling efficiency the parameter  $\tau$  needs to be optimized. An

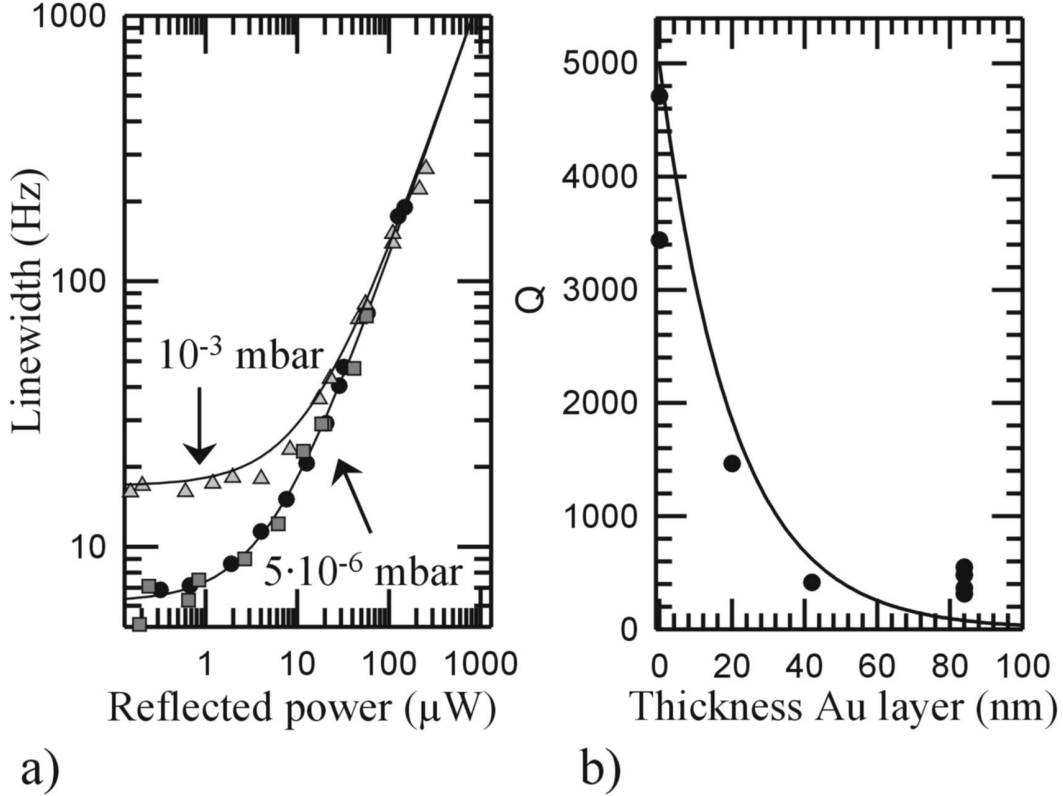


FIG. 5: (a) Dependence of the cantilever's resonance linewidth at full width half maximum with pressure and laser power. The triangles show data taken with a HeNe-laser at moderate pressure of about  $10^{-3}$  mbar, while the circles were taken at minimum pressure of  $5 \times 10^{-6}$  mbar. The squares were taken also at minimum pressure but using a red (670 nm) diode laser instead. Clearly, the linewidth of the cantilever is much smaller at  $5 \times 10^{-6}$  mbar. (b) Mechanical quality factors of different cantilevers with various thicknesses of evaporated gold. The grey line is a guide to the eye.

inspection of eq. (32) shows that optimum cooling is reached for  $\omega\tau = 1$ . In case of thermal bending of the cantilever, the delay time of the light-induced force is given by the time it

takes the thermal energy to diffuse along the cantilever. For a bilayer cantilever consisting of a thin gold layer with thickness  $u_{Au}$  and a silicon layer of thickness  $u_{Si}$ , this thermal diffusion time constant  $\tau_{pth}$  can be approximated by<sup>24,25</sup>

$$\tau_{pth} = l^2 \frac{\rho_{Si} c_{Si} u_{Si} + \rho_{Au} c_{Au} u_{Au}}{\Lambda_{Si} u_{Si} + \Lambda_{Au} u_{Au}}. \quad (37)$$

with  $\rho$  the density  $c$  the specific heat capacity,  $\Lambda$  the thermal conductivity and  $l$  the length of the cantilever. Taking the parameters of the cantilever given above and  $\rho_{Si} = 2.33 \text{ g/cm}^3$ ,  $\rho_{Au} = 19.3 \text{ g/cm}^3$ ,  $c_{Si} = 0.71 \text{ J/(gK)}$ ,  $c_{Au} = 0.128 \text{ J/(gK)}$ ,  $\Lambda_{Si} = 1.48 \text{ W/(cm K)}$  and  $\Lambda_{Au} = 3.17 \text{ W/(cm K)}$  one finds  $\tau_{pth} = 0.5 \text{ ms}$ . With the mechanical resonance frequency of the cantilever of  $f_0 = 7.3 \text{ kHz}$ , a value of  $\omega_0 \tau = 25$  is found. It is interesting to note that  $\omega_0 \tau$  is a function of material thickness alone. The resonance frequency of a multi layer cantilever is given by

$$\omega_0 = \frac{(1.875)^2}{l^2} \sqrt{\frac{1}{u_1 \rho_1 + u_2 \rho_2} \int_{-u/2}^{u/2} E(u - u_0)^2 du} \quad (38)$$

where  $u_0$  denotes the cantilever's neutral stress axis. The Young modulus  $E$  is integrated over the thickness  $u$  of the different cantilever layers<sup>26</sup>. For a cantilever consisting of one layer, eq. (38) simplifies to  $\omega_0 = u/l^2 \sqrt{E/\rho}$  and the corresponding thermal constant is  $\tau_{pth} = l^2/h$  where  $h = \Lambda/(\rho c)$  is the thermal diffusivity. Setting the condition  $\omega \tau = 1$  leads to an optimal thickness  $u_{opt} = h \sqrt{\rho/E}$ . For silicon at room temperature, this optimal thickness is found to be 10 nm with  $h = 8.6 \times 10^{-5} \text{ m}^2/\text{s}$ , the values were found in<sup>27</sup>. This value is far too small for fabrication of free standing silicon structures. However, a diamond resonator with optimized thickness seems feasible. With  $E_{diam} = 1.1 \times 10^{12} \text{ N/m}^2$ ,  $\rho_{diam} = 3200 \text{ kg/m}^3$  and  $h_{diam} = 5.09 \times 10^{-4} \text{ m}^2/\text{s}$ , one finds an optimal thickness of 27.5 nm. A resonator with that thickness and a length of 900 nm would feature a resonance frequency of 100 MHz. For a silicon cantilever, the temperature can be used to tune  $\omega_0 \tau$  since the specific heat  $c$  and the thermal conductivity  $\Lambda$  show strong temperature dependence and a temperature where  $\omega_0 \tau = 1$  can be found. For example, the diffusivity of silicon<sup>27</sup> increases by a factor of 20 from 300 K to 80 K, so placing the cantilever of our experiment at liquid nitrogen temperature of 77 K should allow reaching the optimal condition  $\omega_0 \tau \approx 1$  in contrast to  $\omega_0 \tau \approx 25$  at room temperature.

For radiation pressure induced cooling, the delay time is given by the cavity storage time for a photon<sup>4</sup>  $\tau_R = L/(c(1 - R))$ . With our parameters we find that the cavity storage time is in the range of 0.2 ps and therefore orders of magnitudes smaller than the thermal diffusion time constant. For this reason in this experiment we expect optical cooling to be mostly dominated by photo-thermal effects and not by radiation pressure. In order to obtain the measured value  $\tau_{pth}$  we performed a response measurement of the cantilever's motion driven by a weakly modulated laser light-induced force. The laser intensity of a red diode laser with a wavelength of 670 nm was modulated weakly by modulating the laser current with a signal generator and we used the internal reference of a lock-in (SR 7265). About 5% of the overall intensity was modulated such that the modulation parameter  $\varepsilon$  in eq.(34) was



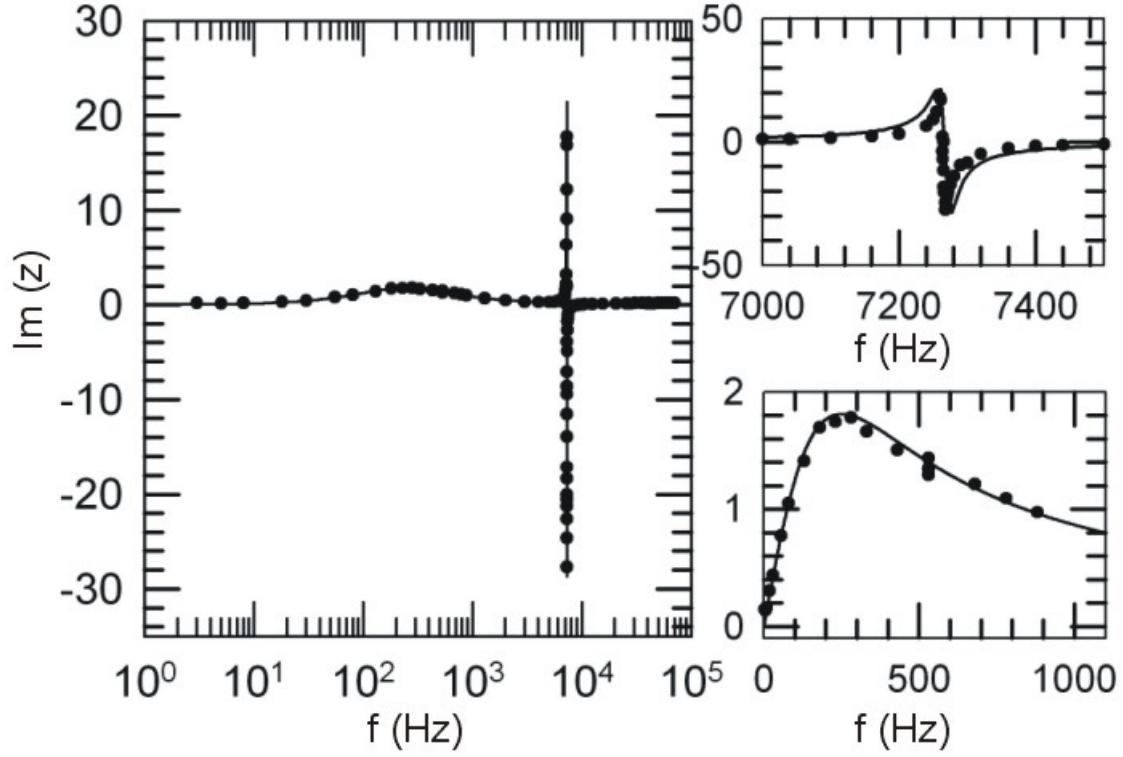


FIG. 6: Response measurement of driven cantilever amplitude. Frequency sweep from 0 to 100 kHz, the small picture above shows a zoom of the region around the cantilever resonance frequency at 7.3 kHz. Inset at the bottom shows a zoom of the enhanced response at  $f=284\text{Hz}$  arising at the frequency where  $\omega\tau = 1$ . The response frequency corresponds to  $\tau_{pth} = 560\mu\text{s}$ .

0.05. The modulation frequency was swept in single steps in the frequency range from DC to 100 kHz. The reflected signal measured at the Si-photodetector was demodulated using the lock-in. We were interested in measuring the imaginary part of the overall amplitude response shown in eq. (36). The measurement of the real part of eq. (36) for low laser amplitude is

$$Re(z_\omega) = \frac{\varepsilon_\omega F_{pth}}{m} \frac{\omega_0^2 - \omega^2(1 + \Gamma\tau)}{[(\omega_0^2 - \omega^2)^2 + \omega^2\Gamma^2](1 + \omega^2\tau^2)} \quad (39)$$

without taking into account the contribution of  $F_{th}$  which is much smaller than  $F_{pth}$ . The real part is always superimposed with the amplitude of the modulated light intensity  $\varepsilon PR$ . This adds a complication in detecting the direct opto-mechanical effect. In contrast, the measurement of the imaginary part

$$Im(z_\omega) = \frac{\varepsilon_\omega F_{pth}}{m} \frac{-\omega[(\omega_0^2 - \omega^2)\tau + \Gamma]}{[(\omega_0^2 - \omega^2)^2 + \omega^2\Gamma^2](1 + \omega^2\tau^2)} \quad (40)$$

is purely dependent on the opto-mechanical response<sup>10</sup>. In the experiment, we found two

different competing forces. A photo-thermal force with a delay time in the range of heat diffusion time was coexistent with the quasi instantaneous radiation pressure force.

The imaginary part shows a characteristic local maximum where the response function  $\omega\tau/(1+\omega^2\tau^2)$  is maximal at the frequency  $1/(2\pi\tau)$ . In a modulated response measurement, one measures an overall phase shift occurring in the system. The phase shift is not only caused by the cantilever's response alone but also includes the phase shifts in the detection apparatus. To solve this technical problem, we devised a measuring procedure cancelling spurious phase shift effects at all frequencies. For each measurement at a given modulation frequency, we first measured the spurious phase shifts by switching off all signal coming from the opto-mechanical response of the cantilever itself. This is obtained when the force gradient  $\nabla F = 0$ , so we tuned the cavity such that the reflectivity was maximum. The phase is then set to zero at the lock-in. In a next step, without changing any other parameter, we detuned the cavity to a regime of maximum  $\nabla F$ . At this point, the imaginary component of the signal is solely originating from the cantilever opto-mechanical response. For each modulation frequency we repeated the procedure explained above. The result is shown in FIG.6. We were able to fit the data with eq. (40) using a combination of two forces acting on the lever. The first is a thermal bending force with a time delay of  $\tau_{pth} = 560 \mu s$ . The second is the quasi-instantaneous ( $\tau \approx 0$ ) radiation pressure that does not contribute here to cooling. The ratio of the forces was found to be  $F_{pth}/F_{rad} = -95$ . On resonance,  $\nabla F_{pth}/(1 + \omega_0^2\tau^2)$  is the contribution of the thermal force to the light-induced frequency shift. Its magnitude is found to be  $95/625=0.15$  smaller than the contribution of  $F_{rad}$  so effects on frequency shift in this experiment were dominated by radiation pressure alone<sup>4</sup>. The modulated experiment shown in FIG. 6 demonstrated convincingly that the observed cooling effects were dominated not by radiation pressure but by a photo-thermal bending force that was 95 times stronger than radiation pressure and had an opposite sign. The value found experimentally for the delay time  $\tau = 560 \mu s$  is in agreement with the prediction of 0.5 ms made with the help of eq. (37). This indicates that a small asymmetry in the thickness of the gold layers on the two faces of the cantilever creates a thermal force opposing the radiation pressure. The imaginary response shows a clear maximum at the cantilever resonance and an enhancement at the the frequency  $f = 1/(2\pi\tau) = 284$  Hz corresponding to the thermal response of the system. We see that the cooling effect at the cantilever's ground mode of 7300 Hz is not optimal, because  $\omega_0\tau \approx 25$  is far from one. As mentioned earlier, placing the lever at 77 K should optimize the cooling to  $\omega_0\tau$  about 1.

## VI. SIMULTANEOUS COOLING OF THE FUNDAMENTAL VIBRATIONAL MODE AND ITS FIRST HARMONIC

In an experiment using a cantilever with a gold coating on one side only, much stronger thermal forces were measured. Here, we used a slightly different cavity arrangement designed to increase the cavity finesse as well as to decrease the size of the laser beam on the microlever.

The light of a red monomode HeNe-laser ( $\lambda = 633$  nm, 1.3mW) was coupled into a

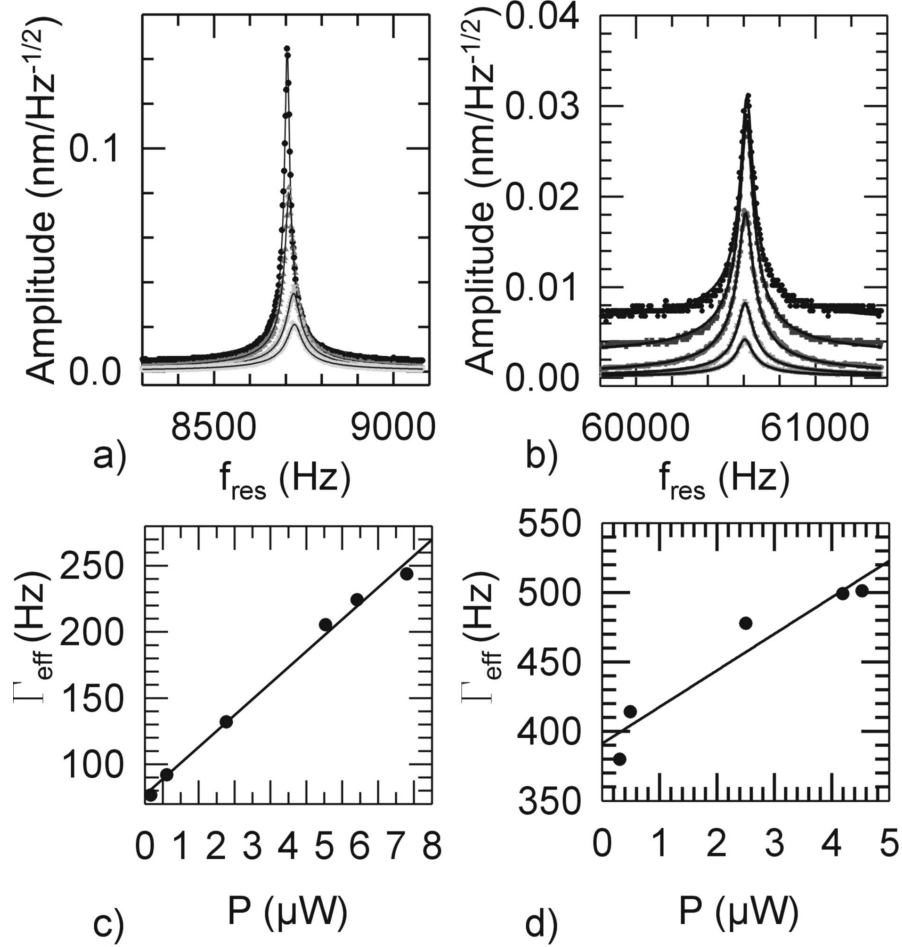


FIG. 7: (a) Cooling behavior of fundamental vibrational mode at 8.7 kHz. Laser powers coupled in the fiber before the cavity are  $0.16\mu\text{W}$  for Brownian peak, then  $2.25\mu\text{W}$ ,  $5.8\mu\text{W}$ ,  $7.6\mu\text{W}$ , corresponding to 300 K, 174 K, 102 K, and 94 K respectively. The fits were made according to eq. (28). The effective damping for the spectra is shown in (c). (b) cooling of first harmonic at 60.6 kHz, laser powers  $0.31\mu\text{W}$ ,  $0.49\mu\text{W}$ ,  $3.14\mu\text{W}$ ,  $4.19\mu\text{W}$ ,  $4.53\mu\text{W}$  corresponding to 300 K, 290 K, 251 K, 240 K, 239 K. The offset of the spectra shows  $1/\sqrt{P}$  dependence and is caused by shot noise of the laser. (c) Effective damping  $\Gamma_{\text{eff}}$  with laser power before cavity for the ground mode at 8.7 kHz.  $\Gamma_{\text{eff}}$  shows linear power dependence according to eq. (14). (d) Effective damping  $\Gamma_{\text{eff}}$  with laser power before cavity for the first harmonics at 60.6 kHz.

single mode fiber (NA=0.13). The fiber end was polished and coated with a reflecting gold

layer of 30 nm (yielding a reflectivity of 70%) to form the first cavity mirror. The divergent beam coming out of the fiber was collimated with a first lens with numerical aperture of  $NA=0.25$  (Geltech glass aspheric lens, diameter 7.2 mm, focal length 11.0 mm), then re-focused on the sample with a second lens identical to the first one. The microscope yielded a gaussian focus on the sample with a  $1/e^2$  diameter of 6  $\mu\text{m}$ . This diameter includes 86% of the gaussian light mode. The sample is a cantilever with length 223  $\mu\text{m}$ , thickness 470 nm, width 22  $\mu\text{m}$ , spring constant  $K = 0.01$  N/m and a gold layer of 42 nm this time on one side only. A simulation of the silicon-gold bilayer system gave a reflectivity of 91%. The cavity finesse defined by the sample and the fiber end was  $F = 8$ . FIG. 7 (a) shows cooling of the cantilever's first mode of vibration at 8.7 kHz from room temperature down to 94 K. The lowest effective temperature of 94 K was reached with the laser intensity of 7.6  $\mu\text{W}$  (power coupled into fiber before first cavity mirror). This is by far not the maximal achievable power with the used laser. However, the cooling was limited by the appearance of instabilities in the static spring constant<sup>18</sup>.

A response measurement with weakly modulated laser done with the same procedure as described in chapter V gave a value for the thermal diffusion time of  $\tau = 760$   $\mu\text{s}$  and a ratio of  $F_{pth}/F_{rad} \approx 4000$ . An interesting point concerning photo-thermal cooling is shown in FIG. 7 (b). The figure shows photo-thermal induced cooling of the cantilever's first harmonic, measured under the same conditions as the cooling of the ground mode shown in FIG. 7 (a). This simultaneous cooling of two modes is very much consistent with the fact that the energy lost to the lowest vibration mode does not feed another mechanical mode of the cantilever but is transferred out of the system.

## VII. PHOTO-THERMAL VERSUS RADIATION PRESSURE COOLING

In this chapter, we compare the lowest temperature reached with photo-thermal cooling and radiation pressure cooling. Both cooling methods are considered in optimal cooling condition at  $\omega_0\tau = 1$ . At present time it is not obvious which method will lead to the lowest temperatures in the quest for quantum ground state cooling of a mechanical resonator. Photo-thermal cooling on one side is always accompanied with optical absorption in the resonator limiting the system's temperature. Its advantages nevertheless are apparent, because the light-induced force can be orders of magnitudes stronger than radiation pressure and the condition  $\omega_0\tau = 1$  can be reached by careful design of the gold layer on the cantilever or else by adjusting the bath temperature as shown in chapter V. In radiation pressure cooling on the other hand, the system still experiences residual absorption heating up the resonator. Additionally, radiation pressure is by far not as strong as photo-thermal forces. To obtain a strong radiation pressure force, the light intensity in the cavity has to be increased considerably leading in turn to increased absorption heat input to the resonator.

First, we address the situation of ideal cooling with radiation pressure without any residual absorptions. As derived in chapter III, the effective temperature is given by eq. (32). In order to reach the minimum effective temperature, the cavity is tuned to the maximal

gradient of radiation pressure<sup>18</sup>

$$\nabla F_{rad,max} \approx \frac{2P_0}{c\lambda} 2\sqrt{R}g^2 \quad (41)$$

where  $P_0$  is the laser power sent on the cavity. This maximal light-induced force gradient occurs at a detuning of  $\lambda/(2\pi g\sqrt{3})$  from a cavity resonance<sup>18</sup>. With this expression and using the cavity storage time  $\tau_{rad} = L/(c(1 - R))$  the minimal effective temperature is found:

$$\frac{T_{eff,rad}}{T} \approx \left( 1 + \frac{1}{1 + \omega_0^2 \tau_{rad}^2} \frac{P_0}{mc^2 \Gamma} g^3 \frac{L}{\lambda/2} \right)^{-1}. \quad (42)$$

Here,  $L$  is the cavity length. For a setup with  $\omega_0 \tau_{rad} = 1$  this simplifies to

$$\frac{T_{eff,rad}}{T} = \left( \frac{P_0}{2mc^2 \Gamma} \frac{L}{\lambda/2} g^3 \right)^{-1} \quad (43)$$

for strong cooling  $T_{eff} \ll T$ . No absorption of light in the mirror was taken into account up to now. Lowest temperatures can be achieved by increasing laser power and finesse, or else by choosing a system with low mass and damping as well as a large cavity length.

Now, we analyze cooling by photo-thermal forces. This effect is not only due to differential thermal expansion in a multilayered composite mirror surface, but can also originate from a non-uniform temperature distribution around the region where light is absorbed. In both cases the effect is not instantaneous and leads to time constants usually much larger than a single pass time of flight of photons through the cavity. The effect can be seen as an effective force that displaces the mirror in proportion to the amount of absorbed laser power. In order to compare photo-thermal forces with radiation pressure we introduce an effective index  $n$  that accounts for a photo-thermal induced force  $F_{pth}$  that would scale like  $nF_{rad}$ , where  $F_{rad} = 2P_0 R/c$  is the force resulting from radiation pressure acting on the mirror. Since the photo-thermal force relies on the absorption  $\alpha$  in the mirror,  $n$  is proportional to  $\alpha$ . For illustration, the factor  $n$  for the doubly-sided gold coated cantilever is -95, while for the cantilever coated on one side only it is 4000.

For better analogy with radiation pressure, where the delay time  $\tau_{rad}$  scales as  $L/(c(1 - R))$ , we give the photo-thermal retardation time in units of  $\tau_{rad}$  such that  $\tau_{pth} = n_\tau \tau_{rad}$ . Physically,  $n_\tau$  represents the thermalization time constant of the mirror in units of  $\tau_{rad}$ . For the first experiment shown in chapter V, this parameter is  $2.8 \times 10^9$ , for the second in chapter VI, it is around  $1.9 \times 10^6$ .

With these definitions, the minimal effective temperature for photo-thermal cooling can be formulated with the help of eq. (32) in the approximation of  $\omega_0 \tau = 1$  and for strong cooling  $T_{eff} \ll T$ :

$$\frac{T_{eff,pth}}{T} = \left( nn_\tau \frac{P_0}{2mc^2 \Gamma} \frac{L}{\lambda/2} g^3 \right)^{-1}. \quad (44)$$

We stress that the effective indexes  $n$  and  $n_\tau$  are purely phenomenological. They are introduced here to allow a direct comparison between photo-thermal and radiation pressure cooling in terms of the ultimate cooling temperatures they yield.

We are now able to compare directly the minimal reachable temperatures and cooling power  $P_{cool}$  accounted for by radiation pressure and photo-thermal forces.

In dark and at thermal equilibrium the lever's mechanical fluctuation dissipates its energy  $k_B T/2$  at a rate  $\Gamma$ . The dissipated power is therefore  $(k_B T/2)\Gamma$  and is in equilibrium with the power that feeds the fluctuation as dictated by the fluctuation-dissipation theorem. When the mechanical resonator is cavity cooled, its vibrational effective temperature is  $T_{eff}$  but at the same time the internal source of mechanical dissipation  $\Gamma$  is still present. In other words the internal mechanical dissipation rate that heats the resonator is still  $\Gamma$ . When the vibrational mode reaches a steady-state at a temperature  $T_{eff}$ , the heat load in the mirror is  $(k_B T_{eff}/2)\Gamma$ . Consequently, in order to maintain a steady state end temperature, the optical cooling extracts energy from the fluctuations in the mirror at a rate

$$P_{cool} = \frac{k_B(T - T_{eff})}{2}\Gamma. \quad (45)$$

Making use of eq. (31), we obtain

$$P_{cool} = \frac{k_B T}{2}\Gamma \left(1 - \frac{\Gamma}{\Gamma_{eff}}\right). \quad (46)$$

For large temperature differences that are typical for efficient cooling we have  $T_{eff} \ll T$  which translates into  $\Gamma_{eff} \gg \Gamma$ . The maximum cooling power is then approximated by  $(k_B T/2)\Gamma$ , which is interestingly still thermal mechanical fluctuation of a resonator in the dark.

Until now, we did not consider any absorptions in the mechanical resonator. Yet, real mirrors always have a finite absorption that acts as a heat source and leads to added fluctuation of the vibrational mode. As a result, it limits the lowest achievable temperature. The absorbed light heats the mirror body to reach a new temperature  $T + \Delta T$  where the excess temperature  $\Delta T = \beta(\alpha P_{mirror})$  is proportional to  $\alpha P_{mirror}$ , the amount of absorbed laser power at the location of the mirror. Here,  $\beta$  is a proportionality factor that translates the absorbed power to an excess temperature and is dependent on the mirror's heat conduction and geometry properties. In a FP cavity, the laser power at the location of the mirror is larger than the laser power outside the cavity by an amount  $P_{mirror} = g P_0$  proportional to the cavity finesse. The excess temperature accounted for by residual absorption in the mirror corresponds to a heating power  $P_{heat} = (k_B \Delta T/2)\Gamma$  of the vibrational mode that ultimately balances the cooling power. The maximum laser power  $P_{max}$  usable before the absorption counteracts the cooling is obtained by equating  $P_{cool} = P_{heat}$  which gives

$$P_{max} = \frac{T}{\alpha \beta g} \left(1 - \frac{\Gamma}{\Gamma_{eff}}\right). \quad (47)$$

In the limit of strong radiation pressure cooling  $\Gamma_{eff} \gg \Gamma$  and cavities with  $\omega_0 \tau = 1$  the relation for minimal temperature eq. (32) for a cavity illuminated with the laser power  $P_{max}$  reads as

$$T_{min,rad} = \left(\frac{P_0}{2mc^2\Gamma} \frac{L}{\lambda/2} \frac{g_{rad}^2}{\alpha_{rad}\beta_{rad}}\right)^{-1}. \quad (48)$$

for radiation pressure cooling and

$$T_{\text{min,pth}} = (n_\tau n \frac{P_0}{2mc^2\Gamma} \frac{L}{\lambda/2} \frac{g_{\text{pth}}^2}{\alpha_{\text{pth}}\beta_{\text{pth}}})^{-1} \quad (49)$$

for photo-thermal cooling. The above derivation gives the means to compare radiation pressure cooling with photo-thermal cooling. One would intuitively think that the photo-thermal effect leads ultimately to heating and that only through radiation pressure cooling one could reach the lowest temperatures. This however needs to be substantiated with numbers as the parameters  $n$ ,  $n_\tau$ ,  $\alpha$  and  $\beta$  can differ in both cooling methods by several decades. We offer here a direct comparison.

Photo-thermal cooling can have a higher cooling rate than radiation pressure cooling as long as  $T_{\text{pth}} < T_{\text{rad}}$ , which translates into the condition

$$\frac{\alpha_{\text{pth}}\beta_{\text{pth}}}{g_{\text{pth}}^2 n_\tau n} < \frac{\alpha_{\text{rad}}\beta_{\text{rad}}}{g_{\text{rad}}^2}. \quad (50)$$

Because the absorption  $\alpha$  scales as  $1/g$ , this can be reformulated as

$$\frac{\beta_{\text{pth}}}{g_{\text{pth}}^3 n_\tau n} < \frac{\beta_{\text{rad}}}{g_{\text{rad}}^3}. \quad (51)$$

In the case of a single experiment with competing cooling mechanisms, we take  $\beta_{\text{pth}} = \beta_{\text{rad}}$  and  $g_{\text{pth}} = g_{\text{rad}}$ . Then the condition for photo-thermal cooling to be superior over radiation pressure cooling is  $n_\tau n > 1$ . Typically,  $n$  lies in the range of several thousand, whereas  $n_\tau$  can be designed to be as large as  $10^{10}$ . To give an example for a mechanical resonator with  $f_0 = 100$  MHz, a delay time of  $1.6 \times 10^{-9}$  s would be optimal. In a cavity with  $g = 9$  ( $R = 0.8$ ) and cavity length  $L = 1$  mm, the photon storage time is only as low as  $1.7 \times 10^{-11}$  s. If the mirror is designed in a way that  $n_\tau = 100$  and  $n = 1000$ , photo-thermal cooling is  $10^5$  times more efficient than radiation pressure cooling.

More generally, if one seeks the most promising mechanism to reach low temperatures, one would have to consider that  $n$  is proportional to the absorption  $n = \xi\alpha$  with the constant  $\xi$  describing the distortion of the mirror with illumination. Then, one needs to compare

$$\frac{\beta_{\text{pth}}}{g_{\text{pth}}^2 n_\tau \xi} \text{ with } \frac{\beta_{\text{rad}}}{g_{\text{rad}}^3}. \quad (52)$$

If we consider the case of  $\beta_{\text{pth}} = \beta_{\text{rad}}$  for the sake of simplicity, one is left with a comparison of  $g_{\text{pth}}^2 n_\tau \xi$  and  $g_{\text{rad}}^3$ . Should the realization of high value of  $n_\tau$  and  $\xi$ , which rely solely on thermal and thermo-mechanical properties of the system, be easier to achieve than a corresponding improvement of the optical  $g$ , then photo-thermal effects would prove to be more promising than radiation pressure to reach low temperatures and approach the oscillator's quantum ground state. The results shown in this work give already a guess of this trend: with a low optical finesse cavity and with adequate thermal properties, we reached temperatures in the range of 10 K in ref<sup>4</sup>, exactly as reported more recently in very high finesse cavities for radiation pressure<sup>8,9</sup>.

## VIII. CONCLUSION

We described a passive photo-thermal cooling mechanism. In our experiments with gold coated micromirrors we were able to cool the thermal vibrations of the mirror from room temperature down to the range of 10 K. The back-action mechanism involving a photo-thermal force time-delayed with respect to any change in mirror position that enables this startling result was described in detail. A theoretical account on the delay time, in our case the time of heat conduction along the mirror, is given and shown to be in good agreement with instantaneous and delayed response measurements. We found that not only the lowest vibrational mode of the mirror is cooled by optical back-action, but also higher modes as well. This result is consistent with the theory which indicates that the energy taken out of any vibrational mode is not transferred into other modes but irreversibly extracted out of the vibrating mirror. A comparison between cooling power of experiments using radiation pressure and photo-thermal cooling is given. The conditions for which photo-thermal cooling leads to lower temperatures than radiation pressure cooling were specified in detail.

We thank T. Hänsch, T. Kippenberg and J. Kotthaus for fruitful discussions. This work was funded by project NOMS KA 1216/2-1 of the Deutsche Forschungsgemeinschaft (DFG). I.F. acknowledges support of the Alexander von Humboldt Foundation.

---

\* Electronic address: Constanze.Metzger@physik.uni-muenchen.de

† Electronic address: Ivan.Favero@physik.uni-muenchen.de

‡ Electronic address: karrai@lmu.de

<sup>1</sup> V. B. Braginsky, and A. B. Manukin, University of Chicago Press, (1977).

<sup>2</sup> V. B. Braginsky, S. E. Strigin, and S. P. Vyatchanin, Phys. Lett. A, **287**, 331, (2001).

<sup>3</sup> V. B. Braginsky, and S. P. Vyatchanin, Phys. Lett. A, **279**, 154, (2001).

<sup>4</sup> C. Metzger, and K. Karrai, Nature, **432**, 1002, (2004).

<sup>5</sup> A. Dorsel, J. D. McCullen, P. Meystre, and E. Vignes, Phys. Rev. Lett., **51**, 1550, (1983).

<sup>6</sup> W. Marshall, C. Simon, R. Penrose and D. Bouwmeester, Phys. Rev. Lett., **91**, 130401, (2003).

<sup>7</sup> S. Gigan, H.R. Böhm, M. Paternostro, F. Blaser, G. Langer, J.B. Hertzberg, K.C. Schwab, D. Bäuerle, M. Aspelmeyer, and A. Zeilinger, Nature, **444**, 67, (2006).

<sup>8</sup> O. Arcizet, P. F. Cohadon, T. Briant, M. Pinard, and A. Heidmann, Nature, **444**, 71, (2006).

<sup>9</sup> A. Schliesser, P. Del’Haye, N. Nooshi, K. J. Vahala and T. J. Kippenberg, Phys. Rev. Lett., **97**, 243905, (2006).



- <sup>10</sup> I. Favero, C. Metzger, S. Camerer, D. König, H. Lorenz, J. P. Kotthaus, and K. Karrai, Appl. Phys. Lett., **90**, 104101, (2007).
- <sup>11</sup> P. F. Cohadon, A. Heidmann and M. Pinard, Phys. Rev. Lett., **83**, 3174, (1999).
- <sup>12</sup> J. Mertz, O. Marti, and J. Mlynek, Appl. Phys. Lett., **62**, 23442346, (1993).
- <sup>13</sup> S. Mancini, D. Vitali, and P. Tombesi, Phys. Rev. Lett., **80**, 688, (1998).
- <sup>14</sup> D. Vitali, S. Mancini, L. Ribichini, and P. Tombesi, Phys. Rev. A, **65**, 063803, (2002).
- <sup>15</sup> D. Kleckner, and D. Bouwmeester, Nature, **444**, 75, (2006).
- <sup>16</sup> F. Marquardt, J. G. E. Harris, and S. M. Girvin, Phys. Rev. Lett., **96**, 103901, (2006).
- <sup>17</sup> M. Poggio, C. L. Degen, H. J. Mamin, and D. Rugar, Phys. Rev. Lett., **99**, 017201, (2007).
- <sup>18</sup> M. Vogel, C. Mooser, and R. J. Warburton, and K. Karrai, Appl. Phys. Lett., **83**, 1337, (2003).
- <sup>19</sup> B. C. Barish, and R. Weiss, Physics Today, **10**, (1999).
- <sup>20</sup> A. Naik, O. Buu, A. D. Armour, A. A. Clerk, M. P. Blencowe, and K. C. Schwab, Nature, **443**, 193, (2006).
- <sup>21</sup> R. Fitzgerald, Physics Today, **11**, 19, (2006).
- <sup>22</sup> R. E. Mihailovich, and N. C. MacDonald, Sensors and Actuators A, **50**, 199, (1995).
- <sup>23</sup> R. Sandberg, K. Molhave, A. Boisen and W. Svendsen, Journal of micromechanics and micro-engineering, **15**, 2249, (2005).
- <sup>24</sup> J. R. Barnes, R. S. Stephenson, C. N. Woodburn, S. J. O'Shea, M. E. Welland, T. Rayment, J. K Gimzewski, and C. Gerber, Rev. Sci. Instr., **65**, 3793, (1994).
- <sup>25</sup> J. K. Gimzewski, C. Gerber, E. Meyer and R. R. Schlittler, Chem. Phys. Lett., **217**, 589, (1994).
- <sup>26</sup> R. Sandberg, W. Svendsen, K. Molhave, and A. Boisen, Journal of Micromechanics and Micro-engineering, **15**, 1454, (2005).
- <sup>27</sup> INSPEC, The Institution of Electrical Engineers, (1988).